




# Seismic fragility functions for Portuguese RC precast buildings

R. Sousa<sup>1</sup> · N. Batalha<sup>2</sup> · V. Silva<sup>3,4</sup> · H. Rodrigues<sup>4</sup> 

Received: 1 July 2020 / Accepted: 9 November 2020 / Published online: 21 November 2020  
© Springer Nature B.V. 2020

## Abstract

Fragility functions are fundamental for the assessment of seismic safety of structures or the loss assessment of a portfolio of assets. The present paper describes a procedure to derive fragility functions representative of Portuguese reinforced concrete precast buildings. This goal was achieved following an analytical methodology considering the result of hundreds of nonlinear static analyses, whose building models reflect both mechanical and geometrical characteristics of the Portuguese industrial building stock. Considering the specificities of this typology, and in particular the connections between the structural members, a recently developed macro-element was employed, which enables the explicit simulation of friction and dowel mechanisms. The fragility analyses considered both structural and non-structural limit states, and the findings indicate a poor seismic performance, even under low seismic demand.

**Keywords** Reinforced concrete · Precast buildings · Non-linear static analyses · Seismic fragility · Risk assessment

## 1 Introduction

The poor seismic performance of reinforced concrete (RC) precast buildings in past earthquakes has been largely documented in the literature (Belleri et al. 2014; Sezen and Whittaker 2006; Liberatore et al. 2013; Magliulo et al. 2014; Bournas et al. 2014; Romão et al. 2013; Babič and Dolšek 2016; Batalha et al. 2019; Dal Lago et al. 2019). These past studies indicate that the structural damage typically occurs at the bottom of the columns with the development of plastic hinges, as well as failures at the

---

✉ H. Rodrigues  
hrodrigues@ua.pt

<sup>1</sup> CDRSP, Polytechnic of Leiria, Leiria, Portugal

<sup>2</sup> CONSTRUCT-LESE, Faculty of Engineering (FEUP), University of Porto, Porto, Portugal

<sup>3</sup> Faculty of Science and Technology, University Fernando Pessoa, Porto, Portugal

<sup>4</sup> RISCO, Civil Engineering Department, University of Aveiro, Aveiro, Portugal

beam-to-column connections due to deficient seismic detailing, namely the absence of steel dowels (Belleri et al. 2015; Magliulo et al. 2014). In addition to the different structural components, important losses result also from damage in non-structural elements, contents, and business interruption. Rodrigues et al. (2018) demonstrated that business interruption, a component that is rarely considered in risk assessment studies, has a significant impact on economic losses, with repercussions that can go beyond the local or regional level.

Damage in industrial buildings is responsible for large social and economic consequences. As noted by Liberatore et al. (Liberatore et al. 2013) and Magliulo et al. (2014), after the 2012 M6.2 (20 May) and the 5.8 (29 May) Emilia-Romagna earthquakes, hundreds of factories suffered severe damage and up to 7000 people lost their jobs due to the direct and indirect effects of the earthquake sequence. The economic losses were estimated as 1 billion EUR on direct losses and about 5 billion EUR on indirect losses due to the disruption of production. In Turkey, after the 1999 M7.6 Kocaeli earthquake, economic losses related with the industrial activities were estimated in more than 30% of the Turkish Gross National Product, corresponding to between 9 and 13 billion USD, decomposed in 5 billion for buildings, 2 billion for industrial facilities, 1.4 billion for infrastructures and the remaining losses for economic losses related with the normalization of the industrial facilities to their normal production levels (Ozerdem and Barakat 2000).

The social and economic losses observed due to the poor seismic behaviour of RC precast industrial buildings emphasize the need to have a better understanding of the seismic performance of this typology, that can be used to improve current construction techniques, assess the vulnerability of existing buildings, and develop efficient retrofitting solutions. Past numerical and experimental studies have contributed to this understanding. For example, by analysing the seismic performance of 65 RC precast buildings in Turkey, Senel and Kayhan (2010) identified the lateral stiffness and ductility as the most critical parameters that govern the seismic response of precast buildings; a conclusion that is coherent with the damage pattern observed after the Kocaeli and Duzce earthquakes of 1999. On the other hand, the field observations (e.g., Babič and Dolšek 2016; Bournas et al. 2013) and fragility analyses conducted by Casotto et al. (2014) on Italian RC precast buildings highlighted the importance of beam-to-column connections, as this structural element is often the main source of structural collapse. According to Casotto et al. (2014), 38% of the industrial building stock in the Tuscany region is likely to suffer extensive damage if a seismic event with a magnitude equal or greater than 6.5 (M<sub>w</sub>) were to occur.

Given the absence of post-earthquake surveys for industrial buildings in Portugal, this study presents an analytical assessment to derive fragility functions considering both structural and non-structural components. Contrarily to what is observed for residential buildings, limited information is available concerning the properties of precast buildings. In Portugal, the study developed for the European Commission in 2013 (Braconi et al. 2013) presents a general description of the main typologies of the industrial building stock. However, this information is insufficient and does not provide detailed data regarding the mechanical, geometric and dynamic properties of the industrial buildings, required to develop representative numerical models. Alternatively, the geometric and mechanical parameters of the Portuguese industrial RC precast buildings collected by Rodrigues et al. (2020) allowed the definition of reliable numerical models that can be used to generate a synthetic model and derive analytical fragility functions. This paper explores also the consideration of both local and global limit states exposing the current limitations regarding the definition of suitable structural limit states for RC precast columns (e.g., Erberik 2008; Crowley et al. 2004).

This study presents the first detailed vulnerability assessment of RC precast structures in Portugal, one of the most representative building classes of the industrial building stock in the country (Crowley et al. 2020). Unlike previous efforts that focused on single structures, the framework presented herein employs statistical models representing a wide range of geometric and material properties to generate hundreds of numerical models. These 3-dimensional models use a novel macro-element to simulate the different types of beam-to-column connections identified in the country, and allow performing nonlinear time history analysis considering a large number of ground motion records. This study explores the propagation of the building-to-building and record-to-record variability in the seismic vulnerability of RC precast structures, resulting in a set of fragility functions that can be used directly in future probabilistic seismic risk assessment at regional or national scale in Portugal. These results also allowed identifying the main drivers of vulnerability in this type of construction, which unlike what was observed in similar structures in Italy that failed mostly due to the beam-to-column connections, in Portugal the factor governing the overall vulnerability is the lack of lateral load capacity of the columns.

## 2 RC precast building in Portugal

The use of RC precast systems in Portugal is mostly applied in the construction of industrial facilities and observed an important grow especially during the 70's decade of the last century (Chastre and Lúcio 2012). Until then, the precast industry in was mainly focused on the construction of elements for slabs and cladding panels. Despite its relatively late appearance, the study carried out by Braconi et al. (2013) indicate that approximately one-third of the current industrial park is composed by RC precast structures. The structural system of these buildings generally consists of large span beams simply supported on columns fixed at the foundation. In the current practice, the connection between these two elements generally comprehends steel dowels, whilst in older buildings it is possible to find cases with no dowels, where the restraints to horizontal movements is ensured only by the friction between the two elements.

The analytical study presented herein relies on the analysis of a population of hundreds of synthetic buildings generated based on the geometric properties gathered from dozens of existing industrial precast RC buildings in Portugal (Rodrigues et al. 2020). Given the absence of a specific structural code for RC precast buildings in Portugal, the definition of the mechanical and geometric properties (see Fig. 1) for each synthetic building resulted from a Monte Carlo sampling process, without any direct or indirect design procedure.

In addition to the statistics regarding the main structural properties, the eventual correlation between variables was investigated so that the numerical models represent, in the best possible manner, the actual industrial building portfolio. In order to reflect this observation, which seem to be naturally related with the evolution of the construction processes, the properties were sampled according to the flowchart presented in Fig. 1.

From the flowchart presented in Fig. 1, it can be observed that the number of bays in the longitudinal direction and the number of storeys (both set equal to one) were fixed during the sampling process. On the other hand, the year of construction, the columns height, the span along the main direction, the columns height/length ratio, the corbel span and the number of bays along the transverse direction were sampled based on the probability distribution functions derived by Rodrigues et al. (2020), and whose main statistical indicators

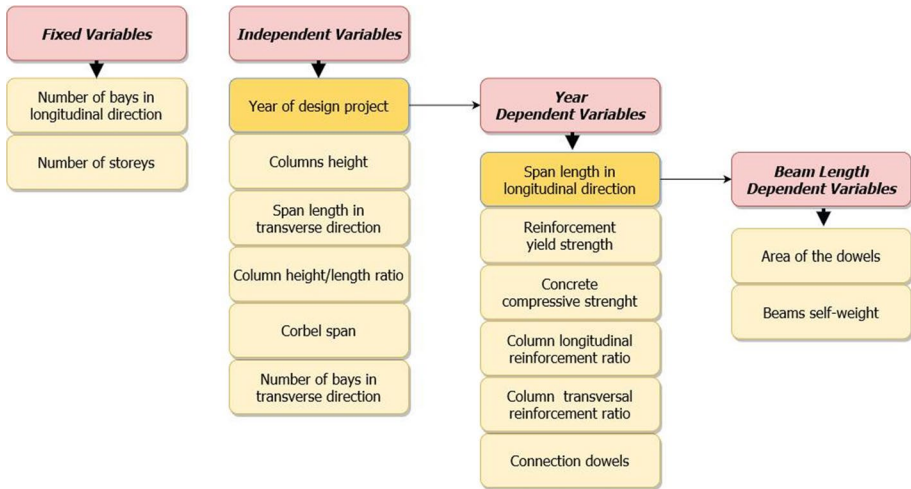


**Fig. 1** Properties considered in the model generation

(mean values, standard deviation, minimum and the maximum value in each variable) are summarised in Table 1.

Finally, a third group of variables were sampled conditioned on the year of construction and the span length along the longitudinal direction (*i.e.*, along the main beams direction). Table 2 presents a summary of the statistics adopted in the model generation procedure, using the year of construction ( $Y$ ), the span length ( $L$ ) in the main direction (longitudinal) and the column length ( $L_c$ ) and the independent variables. The rebars strength vary with the period of construction and this parameter was defined based on the discrete distribution proposed by Rodrigues et al. (2020).

Regarding the expected concrete compressive strength, following the norm NP EN 1992-1-1 (1992) the numerical models assumed a mean value of 8 MPa higher than the characteristic value sampled, whilst for the reinforcement yield strength, the expected value was assumed to be 10% higher than the corresponding characteristic value, as suggested by Priestley et al. (2007).

Considering the larger variability in the building geometric properties when compared to the ones observed in conventional residential buildings (e.g. Furtado et al. 2016; Silva et al. 2015), a total of 1000 industrial buildings were considered in the numerical study.

**Table 1** Statistics of the fixed and independent variables adopted for the generation of the numerical models

Parameter	Mean	STDV	Min	Max	Distribution
Number of bays in transverse direction	8.2	4.8	1	29	Lognormal
Year of design project, $Y$	1990	17.3	1960	2020	Lognormal
Span length in transverse direction (m)	7.6	2.5	4.2	12.5	Lognormal
Column height, $L_c$ (m)	7.7	3.4	3.0	23.0	Lognormal
Column height-to-length ratio	18.1	4.0	6.9	28.9	Normal
Corbel span (cm)	29.4	8.4	15.0	50.0	Lognormal

**Table 2** Statistics of the dependent variables adopted for the generation on the numerical model

Parameter	Mean	$\sigma_E^a$	Min	Max
Span length in the longitudinal direction, L (m)	$\mu = 0.23Y - 437.6$	7.7	5.5	50.0
Longitudinal reinforcement ratio (%)	$\mu = 0.018Y - 34.7$	0.65	0.3	3.7
Transverse reinforcement ratio (%)	$\mu = 0.0043Y - 8.34$	0.17	0.05	0.95
Concrete strength (MPa)	$\mu = 0.52Y - 999$	6.9	12	50
Beam self-weight (kN/m)	$\mu = 0.27L - 0.33$	0.82	2.8	10
Dowel area (mm <sup>2</sup> )	$\mu = 20.3L + 229$	405	50	1608
Length-to-width column ratio	$\mu = 1.885L_C + 0.377$	0.48	1	4

<sup>a</sup> $\sigma_E$  standard deviation

Despite the observed relation between the dowel area and the span in the longitudinal direction, the buildings built before 1990 were modelled without steel dowels. The data collected does not permit the identification of a clear threshold for the generalized use of steel dowels. However, this year seems appropriate as it corresponds to the introduction of a modern seismic code in Portugal (i.e. 1983—RSA 1983), with an additional period of dissemination and implementation in practice. In the buildings with steel dowels, the columns connections to both longitudinal and transverse beams consider two dowels, as these are the typical values found in this type of industrial buildings. Given the lack of specific codes addressing the design of precast RC buildings in Portugal, it was decided to define three sub-classes based on the year of construction, as an important fraction of the mechanical and geometric properties depend on the year of construction (see Table 2). The three groups were defined as Pre-code (1960–1980), Moderate-code (1980–2000) and Post-code (2000–2020) and are represented in Fig. 2.

### 3 Modelling assumptions

The seismic assessment was carried out through nonlinear static analysis of 3D models along the two main directions of the buildings using the structural analysis software OpenSees (McKenna 2011), which features element formulations and material constitutive relationships highly validated in the literature. As described in more detail in the following sections, each of the 1000 different buildings was analysed along the two main directions and features two alternative beam-to-column connections—an explicit macro-model and a simple pinned connection approach.

Considering that the damage tends to concentrate at the bottom of the columns or at the beam-to-column connections (Liberatore et al. 2013; Magliulo et al. 2014; Batalha et al. 2019), the columns were modelled with force-based nonlinear beam elements whilst both longitudinal and transverse beams were modelled with elastic elements, following an approach commonly adopted for precast RC buildings (e.g., Fajfar 1999; Brunesi et al. 2015). The number of integration points per column vary according to the properties of the columns and were defined so that the integration weight of the extreme integration point approaches the expected equivalent plastic hinge length, following the recommendations from Sousa et al. (2018).

In terms of the material properties, the concrete was modelled with the Concrete01 model, based on the Kent-Scott-Park concrete model (Kent and Park 1971; Scott and

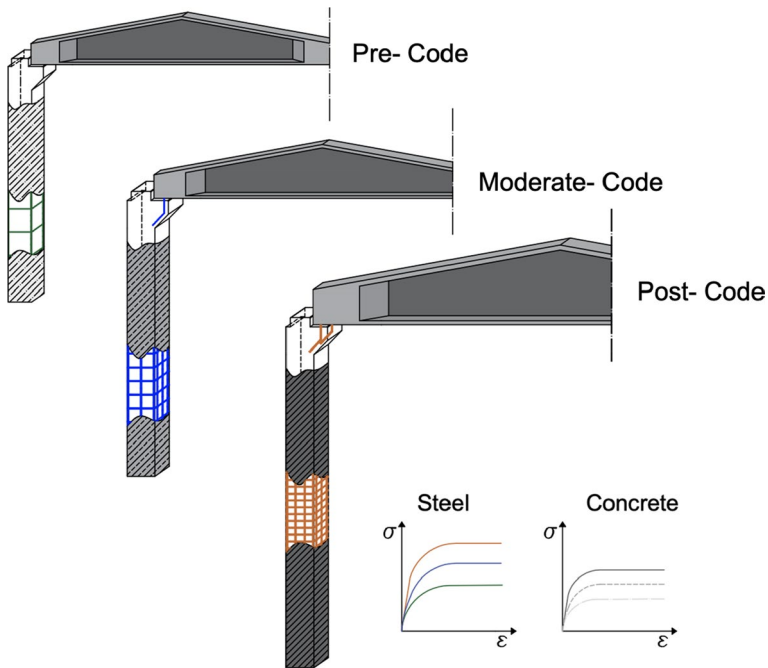


**Fig. 2** Schematic illustration of the considered sub-classes of RC precast buildings

Priestley 1982) whereas the longitudinal reinforcement was simulated with the Steel02 model, based on the Giuffrè–Menegotto–Pinto model (Menegotto and Pinto 1973).

The variations in the beam-to-column connections were simulated through a macro-element proposed and validated against experimental tests by Sousa et al. (2020) which is able to describe the main mechanisms present in conventional beam-to-column RC precast connections, namely the friction between the different elements, the steel dowels effects (when present) and the neoprene pad (always considered in the model). This macro-element consists of a zero-length element (i.e., the end node of the beam and column have the same coordinates), that includes the contribution of the different systems through different springs that are aligned in series or in parallel, depending on the manner these are activated in real structures. The spring arrangement, illustrated in Fig. 3, is defined for both horizontal directions, while the rotations along the three main directions are released. This model was adopted in the connections of both longitudinal and transverse beams.

It is recognized that the presence of heavy cladding systems can change the dynamic behaviour and the collapse mechanisms (Magliulo et al. 2014, 2015; Belleri et al. 2016) of precast buildings. Yet, as noted by Brunesi et al. (2015), their contribution is mostly relevant during elastic response phase. Hence, for the present case, the infill walls were assumed to have a low mass and therefore, the effects of cladding panels and their interaction with the main structure were not considered in these analyses. Regarding the roof claddings, if design with enough in-plane stiffness and proper connections, these can play an important role in the seismic performance of precast frame structures (Dal Lago et al. 2019), ensuring a rigid diaphragm behaviour. However, based on field observations and expert opinion, it seems evident that in the common construction practice in industrial buildings the roof is typically light and flexible. Therefore, the strength and stiffness of the

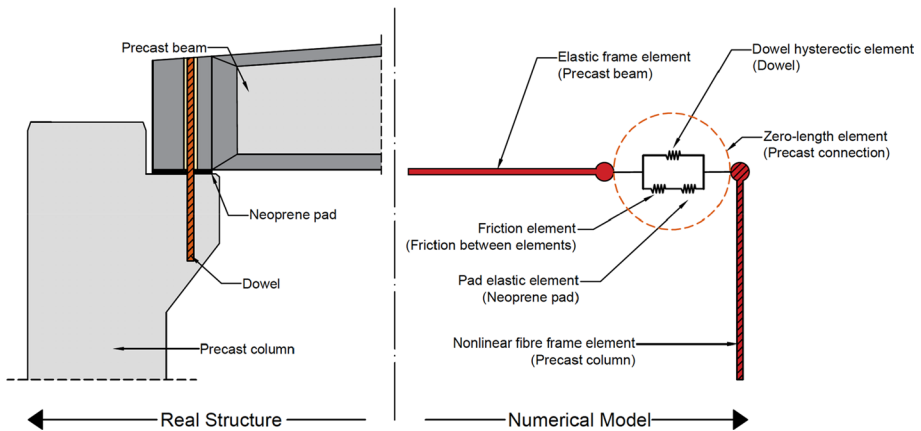


**Fig. 3** Numerical model adopted to simulate the behaviour of the beam-to-column connections

cladding system was neglected and an additional gravity load of  $0.65 \text{ kN/m}^2$  was distributed on the beams to simulate the self-weight of the roof.

The seismic performance of each building was assessed through nonlinear adaptive static analyses. In a nutshell, in these analyses the building is subject to a progressive increase in horizontal loading (displacements in the present case) until it reaches a level of deformations that leads to the local or global instability of the building. With respect to conventional nonlinear static analysis, the adaptive approach accounts for the contribution of higher modes (not relevant in structures controlled by the fundamental mode, as the ones analysed herein) and the modification in the dynamic properties of the buildings with the progression of damage.

#### 4 Characterization of the seismic behaviour

In order to understand the contribution of the different mechanisms to the seismic behaviour of these structures, every building was simulated with three variants of beam-to-column connections: (1) pinned connection, (2) connection with dowels and (3) connection without dowels. The latter two cases were simulated with the macro-model described in the previous section. As expected, this variation leads to distinct seismic behaviours of the overall structure. As illustrated in Fig. 4, in the absence of steel dowels (case 3), the seismic coefficient (defined as the ratio between the lateral strength and the self-weight of the building) is largely reduced to maximum values of about 0.1.

Another relevant observation regards the large dispersion of the capacity curves, reflecting the much larger variability of the building properties when compared to conventional residential buildings. In industrial precast buildings both global (columns height and beam spans) and local (columns cross-section and reinforcement detailing) properties may vary significantly depending on the expected building use. This observation points to the eventual need to define different classes or sub-classes of precast buildings. A possible option to assess the need to consider sub-classes of buildings is to evaluate the number of sampled buildings required to reach a stable mean response. Figure 5 represents the relative error of 25 different realizations considering random samples of buildings with increasing size (from 20 to 1000), with respect

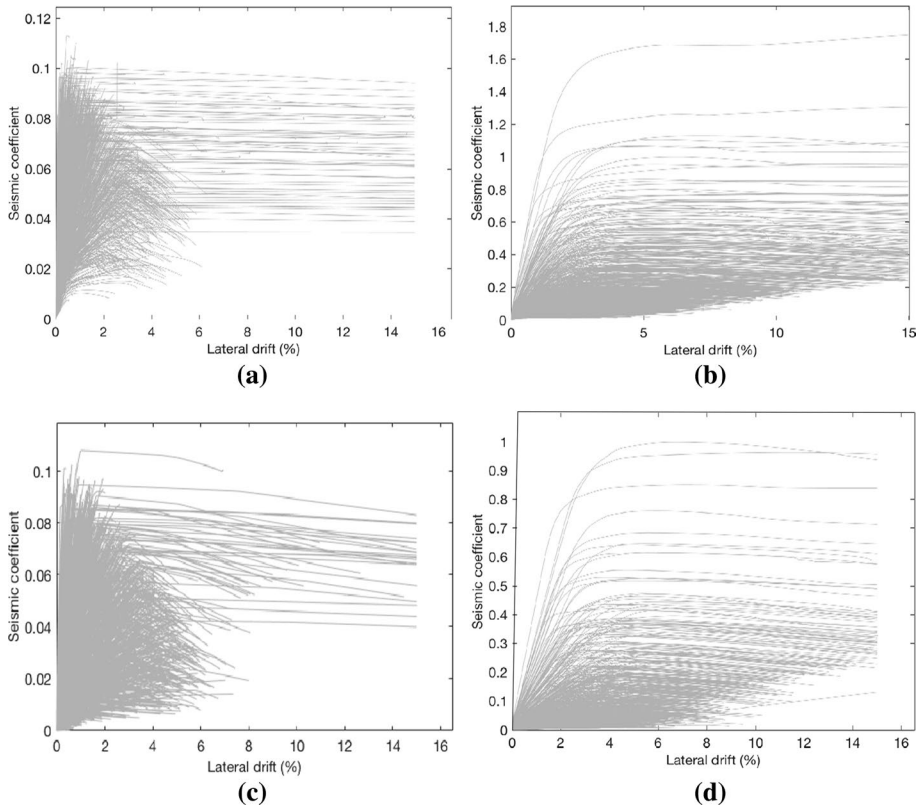


**Fig. 4** Relations between lateral drift and seismic coefficient along **a** X-direction without dowels, **b** X-direction with dowels, **c** Y-direction without dowels and **d** Y-direction with dowels

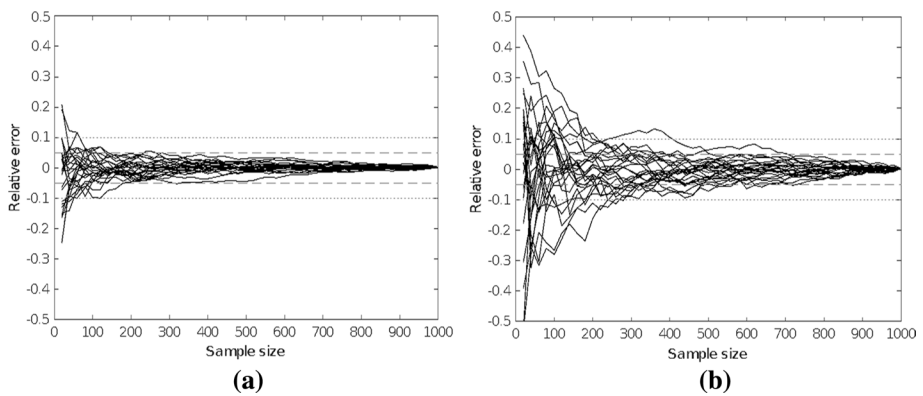


**Fig. 5** Evolution of the mean relative error in terms of: **a** spectral displacement, **b** spectral acceleration for 25 different realizations of increasing sample size



**Fig. 6** Histogram of the lateral drift values measured at the maximum base shear for 1000 synthetically generated structures assuming a pinned beam-to-column connection

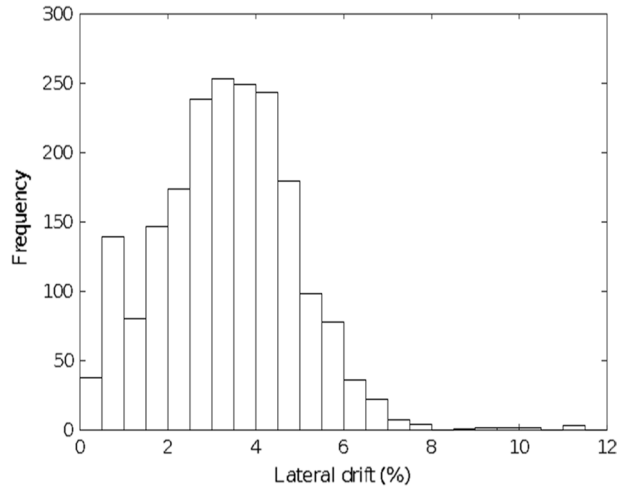


**Table 3** Columns deformation limit states found in previous studies

	Type of analysis	Yield drift	Ultimate drift (%)
Fischinger et al. (2008)	Experimental	2.8%	8
Casotto (2013)	Numerical		4
Bellotti et al. (2009)	Experimental	–	3
Crowley et al. (2004)	Numerical		4

to the mean engineering demand parameter (*EDP*) obtained with 1000 samples. These plots measure the relative error in terms of spectral displacement and spectral acceleration associated with the instant where the maximum base shear is attained. To reduce the level of structural uncertainty, only buildings with pinned connections were considered.

The results show that a sufficiently low relative error is achieved only when the number of samples is approximately 300 or 800 buildings, depending on the chosen *EDP* (i.e. spectral displacement or spectral acceleration, respectively). Moreover, these results indicate that despite the large variation of the seismic coefficient, the columns lateral drift at maximum shear seem to present a lower variation. Nonetheless, a large dispersion in the columns lateral drifts is still observed (see Fig. 6), stressing the need to consider sub-classes of buildings, reducing this way the variability within each class. In addition to the relatively high lateral drift values when compared to common (cast in place) RC framed buildings, the results also show a large dispersion in the drift values, highlighting the current difficulties in the definition of appropriate limit states for precast structures, as recently noted by Casotto et al. (2015), and demonstrated by the variability found in previous studies (see Table 3).

## 5 Fragility analyses

### 5.1 Definition of building classes and seismic input

Following the results presented in the previous section, three different classes of buildings were considered, reducing the variability of the structural properties within each group. Each of these groups includes 300 buildings (analysed in both directions), which was found to be enough to obtain convergence in the structural response. Only buildings built after 1990 were assumed to have steel dowels at the beam-to-columns connections. This implies that the three groups will reflect different dowel properties: (1) no dowels for pre-code buildings, (2) half of the buildings with dowels for moderate-code buildings and (3) all buildings with dowels for post-code buildings.

The seismic performance of every building was assessed considering a dataset with 250 records covering the Mediterranean region, which is consistent with the region under study. Considering the large period of vibration characteristic of this type of structures, all the records were scaled, considering a maximum factor of 3.5, in order to reach seismic intensities capable of causing the structures to collapse. The scaled acceleration spectra together with the histograms of the peak ground acceleration and spectral acceleration at the average period of the synthetic building portfolio ( $T=1.7$  s) are presented in Figs. 7b and 8, respectively. The latter are merely indicative, as the fundamental period of vibration of the buildings shows a large dispersion, as illustrated in Fig. 7a. It is noted that the magnitude and dispersion of the fundamental periods are essentially independent of the period of construction. The seismic performance of each building was then accessed through the N2 method (Fajfar 1999), as suggested in the Eurocode 8, along the two directions of the buildings.

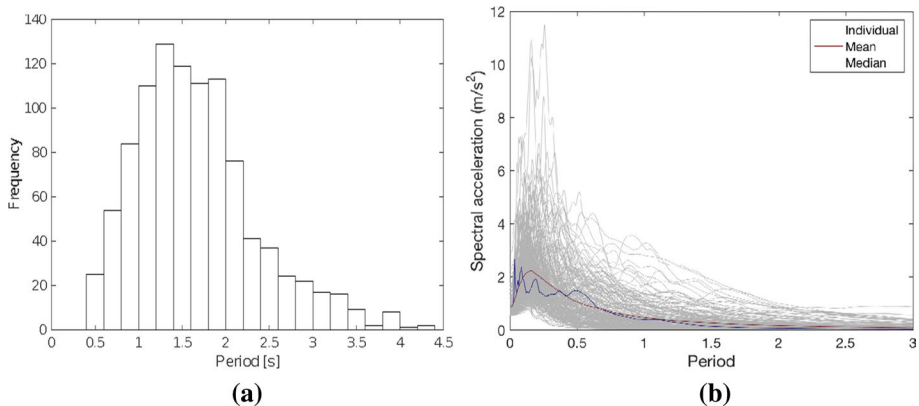


**Fig. 7** Effect of buildings dynamic properties in the seismic demand: **a** histogram of the average period of both building directions and **b** scaled spectral accelerations considered as seismic input

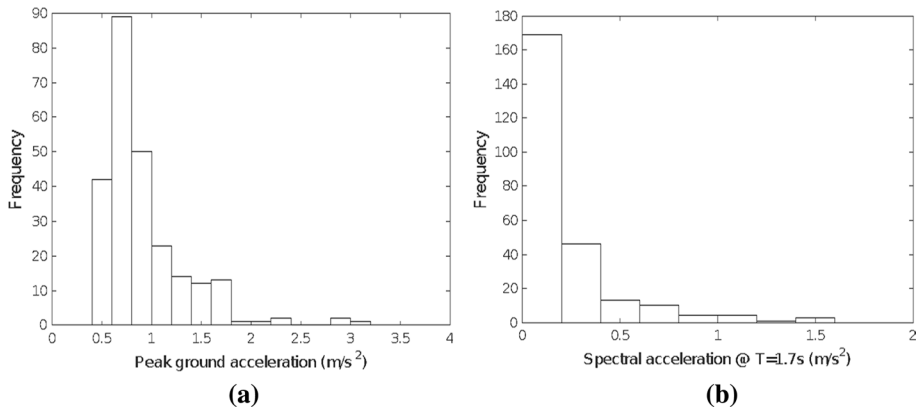


**Fig. 8** Histograms of **a** peak ground acceleration, **b** spectral acceleration at  $T=1.7$  s of the selected ground motion records

## 5.2 Definition of limit states

A key step in the derivation of fragility functions involves the definition of the thresholds for the EDPs, representing different damage levels. For the fragility analyses presented herein, two limit states were considered: damage control and collapse prevention, associated with both structural and non-structural components.

In terms of structural elements, the assessment was focused on the response of both columns and beam-to-column connections. An initial attempt was made to consider deformation thresholds recommended in past studies (e.g., Furtado et al. 2016; Beilic et al. 2017). However, as illustrated in Fig. 6, the dispersion obtained in the columns lateral drifts precluded the consideration of such limit states, as some buildings reached the near collapse drift limits (i.e. 3%) in early stages of lateral load, whilst others reached damage limitation drifts (i.e. 1%) already in the post-peak (softening) response. It is thus clear that further research in this topic is necessary, possibly by defining a drift limit dependent on some structural properties instead of considering generalized thresholds for all precast RC buildings.

Given these constraints, alternative limit states for the columns related to the global capacity curve were considered. For damage limitation, a threshold was set to the attainment of 60% of the maximum base shear capacity ( $F_{max}$ ). For collapse prevention, two thresholds were defined: 1) a drop of the base shear capacity to  $0.8 F_{max}$  or 2) a global drift corresponding to 4 times the displacement associated with the damage limitation limit state (which is equivalent to a ductility value of 4). The collapse prevention limit state is attained when one of these criteria is achieved. Given that the limit states are defined as a function of the maximum lateral strength, specific limit states are defined for each building and direction.

The displacement capacity of the beam-to-column connections was defined as the relative displacement between the top of the columns and the adjacent beams. Limits of 3 cm and 8 cm for the damage limitation and collapse prevention, respectively, were assumed, as suggested by Cornali et al. (2017). Since the column and connection limit states act in series, the attainment of a structural limit state is dictated by the one

**Table 4** Limit states adopted for the different elements and performance levels

<i>Structural limit states</i>	
Columns	
Collapse prevention	80% drop $F_{max}$
Damage limitation	60% $F_{max}$
Connection	
Collapse prevention	8 cm relative displacement (Cornali et al. 2017)
Damage limitation	3 cm relative displacement (Cornali et al. 2017)
<i>Non-structural limit states</i>	
Claddings	
Collapse prevention	4 cm relative displacement between cladding connections (Cornali et al. 2017)
Damage limitation	1 cm relative displacement between cladding connections (Cornali et al. 2017)

that occurs first. This condition implies that the performance of the columns is known regardless of the capacity of the connection. For this reason, the identification of the 80% and 60% of  $F_{max}$  was carried out based on the results of nonlinear analysis considering a pinned connection between the columns and beams.

Regarding the non-structural components, the performance was evaluated through the control of the relative deformation between the top and bottom connections of the cladding panels, as suggested by Cornali et al. (2017). Despite the absence of cladding panels in the numerical models, the damage in the panels was simulated through the measurement of the lateral deformation of the columns. Assuming a common configuration of the claddings (i.e. horizontal panels with 3 m height), limits of 1 cm and 4 cm of relative displacement for the damage limitation and collapse prevention limit states, respectively, can be approximated to 0.3% and 1.3% of columns drift. A summary of the adopted structural and non-structural limits states is presented in Table 4.

### 5.3 Fragility curves

The fragility functions presented in this section were derived using a nonlinear static procedure carried out on 900 synthetically generated numerical models, equally distributed across the 3 different building classes (i.e. Pre-code, Moderate-code and Post-code). Considering that each building was analysed along the two directions, the seismic intensity associated with each building was defined based on the minimum of the one obtained for each direction. Despite the results being discussed on the bases of averaged spectral acceleration between half and two times the average elastic period of all the buildings ( $T=1.7$  s), the results were derived, and are presented at the end of this section, also in terms of spectral acceleration at the same period of vibration.

The results presented in Fig. 9 show the response of the individual industrial buildings together with the associated lognormal cumulative distribution associated with the structural limit states (i.e. damage limitation and collapse prevention) for the three building classes, disaggregated in terms of conditioning mechanism (columns or connections). Each point in the plots represents the ratio of buildings within each class that reached a given limit state under analysis for each ground motion record, represented by the associated averaged spectral acceleration.

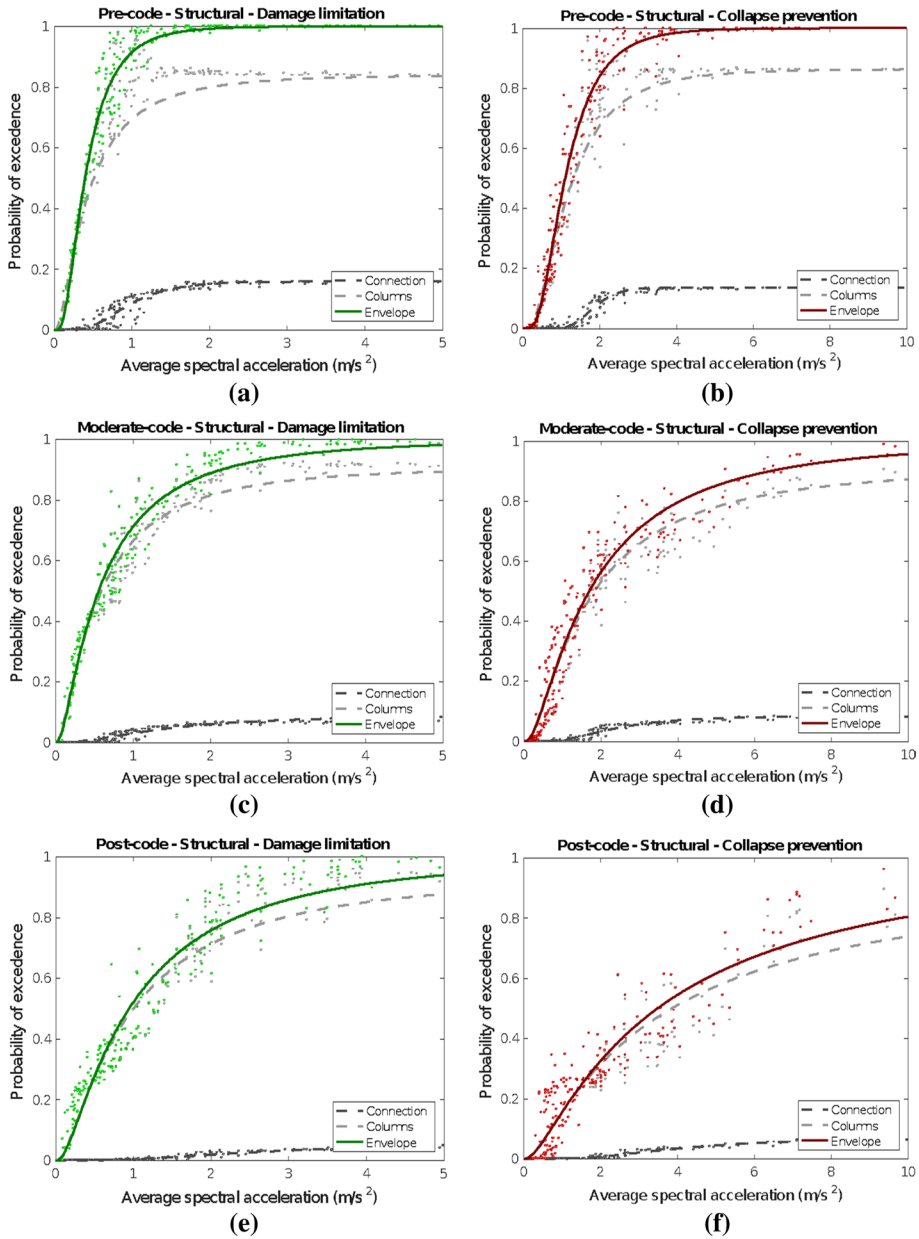


**Fig. 9** Structural fragility functions for building models for **a** pre-code design for damage limitation state, **b** pre-code design for collapse prevention limit state, **c** moderate-code design for damage limitation state, **d** moderate-code design for collapse prevention limit state, **e** post-code design for damage limitation state, **f** post-code design for collapse prevention limit state

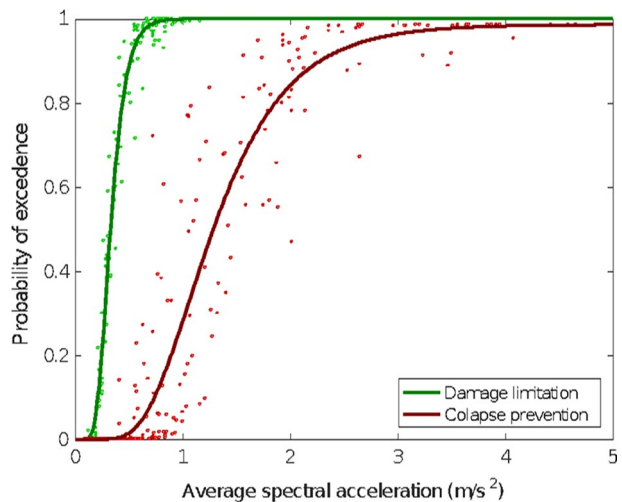
The results confirmed that, in the presence of dowels, the response is generally controlled by the columns, while the failure at the connections is observed only in marginal cases (bottom plots in Fig. 9). On the contrary, in the absence of steel dowels (in all

the Pre-code buildings and a fraction of the Moderate-code buildings), a larger number of buildings exhibit vulnerabilities at the connection level. The reason for this distinct behaviour relies on the reduced lateral strength of the columns analysed in this study. In the presence of particularly slender columns, the response tends to be governed by the columns' behaviour and the friction strength at the connection level is often enough to sustain the maximum shear forces developed in the columns. For the cases where the columns are more robust (with a local seismic coefficient higher than about 0.1), the friction at the connection is not enough to sustain the lateral loads and the beams experience large lateral displacements.

For what regards the non-structural components, all the typologies presented similar average spectral accelerations for both limit states and, therefore the results reflect the behaviour of the entire portfolio of buildings (see Fig. 10). The reduced variation observed among the different groups results from the columns slenderness (and hence the buildings initial lateral stiffness) being independent of the year of construction, as described in Sect. 2. Furthermore, given the low deformation level associated with these limit states, the damage in the cladding appears to be independent of the type of structural failure.

Figure 11 summarizes the fragility curves for the different typologies expressed both in terms of average spectral acceleration at the elastic period of vibration. For both damage limitation (dashed lines) and collapse prevention (full lines) structural limit states, it is possible to observe an improvement in the seismic capacity with the year of construction of the buildings, evaluated in terms of code compliance (pre-, moderate and post-code). On the other hand, in what regards performance of the non-structural components, the year of construction appears to have a negligible importance. The most relevant statistic parameters of the fragility curves are presented in Tables 5 and 6, for average spectral accelerations and spectral accelerations at the averaged elastic period of the population of buildings, respectively. The statistical parameters of the lognormal distributions present an acceptable correlation with the individual data with correlation values  $r^2$  higher than 0.9 for all of the curves presented in this paper.

**Fig. 10** Non-structural fragility functions for building models from all ages



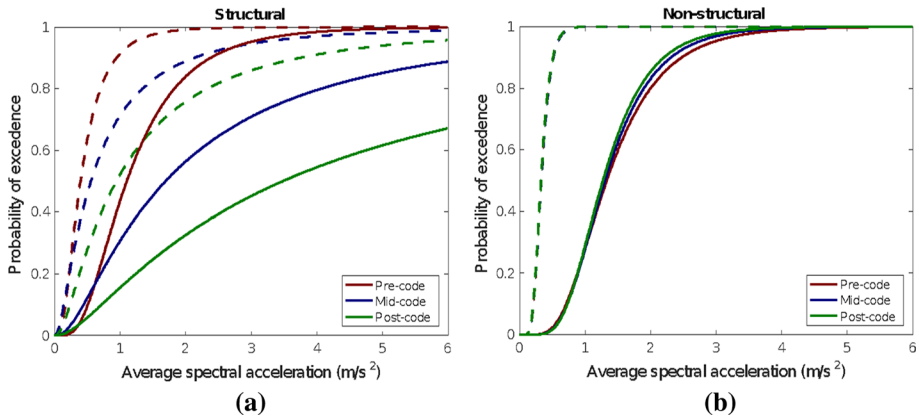


**Fig. 11** Comparison of the fragility curves associated with the damage limitation (dashed lines) and collapse prevention (full lines) obtained for different typologies, **a** for structural performance limit states, **b** for non-structural performance limit states

**Table 5** Summary of the statistics associated with the fragility functions in terms of averaged spectral accelerations in  $m/s^2$

Limit state	Pre-code		Moderate-code		Post-code	
	Mean	SD	Mean	SD	Mean	SD
<b>Structural</b>						
Damage limitation	0.50	0.14	0.97	1.87	1.69	6.16
Collapse prevention	1.33	0.76	2.92	16.54	7.35	190.00
<b>Non-structural</b>						
Damage limitation	0.35	0.02	0.35	0.02	0.35	0.02
Collapse prevention	1.50	0.60	1.44	0.46	1.40	0.40

**Table 6** Summary of the statistics associated with the fragility functions in terms of spectral accelerations at the elastic period in  $m/s^2$

Limit state	Pre-code		Moderate-code		Post-code	
	Mean	SD	Mean	SD	Mean	SD
<b>Structural</b>						
Damage limitation	0.50	0.15	0.98	2.07	1.76	7.62
Collapse prevention	1.34	0.84	3.17	23.01	9.03	385.2
<b>Non-structural</b>						
Damage limitation	0.35	0.02	0.35	0.02	0.35	0.02
Collapse prevention	1.52	0.69	1.46	0.53	1.41	0.44

## 6 Conclusions

This study presents the development of fragility curves for precast RC buildings representative of the Portuguese industrial building stock, reflecting both structural and

record-to-record variability. To this end, a portfolio of hundreds of synthetic buildings was generated mimicking the material and geometric properties found in Portugal. Recognizing that an important fraction of the structural properties is year-dependent, three typologies of industrial buildings were defined based on the period of construction.

Considering the concentration of damage at the beam-to-column connections observed in previous earthquakes, the numerical models employed in this study feature a macro-element capable to simulate the different systems at these connections in an independent manner, namely the contribution of the friction, steel dowels (if present) and neoprene pad. The three-dimensional models were subjected to nonlinear static analysis to assess the main sources of damage.

The fragility curves expressed in terms of spectral acceleration showed that large structural and non-structural damage are expected for low levels of seismic intensity. This apparent vulnerability results essentially from the high slenderness of the columns, that reach its maximum lateral strength for very low levels of lateral load. Even in the building typologies that do not feature steel dowels at the beam-to-column connections, only a small portion of the buildings (around 15%) presented structural issues at the connections. These results contrast with the recent study conducted for Italy (Casotto et al. 2014), in which a larger amount of buildings showed structural issues at the connections, although, overall, the buildings feature higher seismic resistance.

The results from this study contribute to the understanding of earthquake risk in Portugal and can be used directly in the assessment of earthquake damage or economic losses considering specific earthquake scenarios or probabilistic seismic hazard. The methodology and numerical models described herein are also relevant for the assessment of the seismic fragility of precast buildings in other regions.

**Acknowledgements** This work was financially supported by Project POCI-01-0145-FEDER-028439 —“SeismisPRECAST Seismic performance ASSESSment of existing Precast Industrial buildings and development of Innovative Retrofitting sustainable solutions” funded by FEDER funds through COMPETE2020—Programa Operacional Competitividade e Internacionalização (POCI) and by national funds (PIDDAC) through FCT/MCTES. The second author acknowledged to FCT—Fundação para a Ciência e a Tecnologia namely through the PhD grant with reference SFRH/BD/139723/2018.

## References

- Babič A, Dolšek M (2016) Seismic fragility functions of industrial precast building classes. *Eng Struct* 118:357–370. <https://doi.org/10.1016/j.engstruct.2016.03.069>
- Batalha N, Rodrigues H, Varum H (2019) Seismic performance of RC precast industrial buildings—learning with the past earthquakes. *Innov Infrastruct Solut* 4:4. <https://doi.org/10.1007/s41062-018-0191-y>
- Beilic D, Casotto C, Nascimbene R, Cicola D, Rodrigues D (2017) Seismic fragility curves of single storey RC precast structures by comparing different Italian codes. *Earthq Struct* 12(3):359–374. <https://doi.org/10.12989/eas.2017.12.3.359>
- Belleri A, Brunesi E, Nascimbene R, Pagani M, Riva P (2014) Seismic performance of precast industrial facilities following major earthquakes in the Italian territory. *J Perform Constr Facil* 29:40
- Belleri A, Brunesi E, Nascimbene R, Pagani M, Riva P (2015) Seismic performance of precast industrial facilities following major earthquakes in the Italian territory. *J Perform Constr Facil* 29(5):04014135. [https://doi.org/10.1061/\(ASCE\)CF.1943-5509.0000617](https://doi.org/10.1061/(ASCE)CF.1943-5509.0000617)
- Belleri A, Torquati M, Marini A, Riva P (2016) Horizontal cladding panels: in-plane seismic performance in precast concrete buildings. *Bull Earthq Eng* 14(4):1103–1129. <https://doi.org/10.1007/s10518-015-9861-8>
- Bellotti D, Bolognini D, Nascimbene R (2009) Response of traditional RC precast structures under cyclic loading. <https://doi.org/10.3383/es.2.2.1>



- Bournas D, Negro P, Taucer FF (2013) Performance of industrial buildings during the Emilia earthquakes in Northern Italy and recommendations for their strengthening. *Bull Earthq Eng* 12(5):2383–2404. <https://doi.org/10.1007/s10518-013-9466-z>
- Bournas DA, Negro P, Taucer FF (2014) Performance of industrial buildings during the Emilia earthquakes in Northern Italy and recommendations for their strengthening. *Bull Earthq Eng* 12(5):2383–2404. <https://doi.org/10.1007/s10518-013-9466-z>
- Braconi A, Osta A, Dall'Astra A, Leoni G, Möller S, Hoffmeister B, Karamanos S, Varelis G, Alderighi E, Coscetti C, Salvatore W, Gracia J, Bayo E, Mallardo R, Bianco L, Filipuzzi P, Vasilikis D, Tsintzos P, Estanislau S et al (2013) Prefabricated steel structures for low-rise buildings in seismic areas (Precas-teel). Brussels
- Brunesi E, Nascimbene R, Bolognini D, Bellotti D (2015) Experimental investigation of the cyclic response of reinforced precast concrete framed structures. *PCI J* 1:5. <https://doi.org/10.15554/pcij.03012.015.57.79>
- Casotto C (2013) Seismic vulnerability of Italian RC precast industrial structures, p 68
- Casotto C, Silva V, Crowley H, Pinho R, Nascimbene R (2014) Scenario damage analysis of RC precast industrial structures in Tuscany, Italy. In: Second European conference on earthquake engineering and seismology, 2014, pp 1–12. <https://doi.org/10.13140/2.1.1725.5683>
- Casotto C, Silva V, Crowley H, Nascimbene R, Pinho R (2015) Seismic fragility of Italian RC precast industrial structures. *Eng Struct* 94:122–136. <https://doi.org/10.1016/j.engstruct.2015.02.034>
- Chastre C, Lúcio V (2012) Estruturas Pré-moldadas no Mundo—Aplicações e Comportamento Estrutural, Fundação d
- Cornali F, Belleri A, Marini A, Riva P (2017) Influence of modelling assumptions in the expected loss evaluation of a precast industrial building. *Procedia Eng* 199:3510–3515. <https://doi.org/10.1016/j.proeng.2017.09.499>
- Crowley H, Pinho R, Bommer J (2004a) A probabilistic displacement-based vulnerability assessment procedure for earthquake loss estimation. *Bull Earthq Eng* 2:173–219
- Crowley H, Pinho RUI, Bommer JJ (2004) A probabilistic displacement-based vulnerability assessment procedure for earthquake loss estimation, pp 173–219
- Crowley H, Despotaki V, Rodrigues D, Silva V, Toma-Danila D, Riga E, Karatzetou A, Zugic Z, Sousa L, Ozcebe S, Gamba P (2020) Exposure model for European seismic risk assessment. *Earthq Spectra*. <https://doi.org/10.1177/8755293020919429>
- Dal Lago B, Silvia L, Fabio B (2019) Diaphragm effectiveness of precast concrete structures with cladding panels under seismic action. *Bull Earthq Eng* 17(1):473–495. <https://doi.org/10.1007/s10518-018-0452-3>
- Erberik MA (2008) Fragility-based assessment of typical mid-rise and low-rise RC buildings in Turkey. *Eng Struct* 30(5):1360–1374
- Fajfar P (1999) Capacity spectrum method based on inelastic demand spectra. *Earthq Eng Struct Dyn* 28(9):979–993. [https://doi.org/10.1002/\(SICI\)1096-9845\(199909\)28:9%3C979:AID-EQE850%3E3.0.CO;2-1](https://doi.org/10.1002/(SICI)1096-9845(199909)28:9%3C979:AID-EQE850%3E3.0.CO;2-1)
- Fischinger M, Kramar M, Isakovic T (2008) Cyclic response of slender RC columns typical of precast industrial buildings. *Bull Earthq Eng* 6:519–534. <https://doi.org/10.1007/s10518-008-9064-7>
- Furtado A, Costa C, Arêde A, Rodrigues H (2016) Geometric characterisation of Portuguese RC buildings with masonry infill walls. *Eur J Environ Civ Eng* 20(4):396–411. <https://doi.org/10.1080/19648189.2015.1039660>
- Kent DC, Park R (1971) Flexural members with confined concrete. *J Struct Div* 97(7):1969–1990
- Liberatore L, Sorrentino L, Liberatore D, Decanini L (2013) Failure of industrial structures induced by the Emilia (Italy) 2012 earthquakes. *Eng Fail Anal* 34:629–647. <https://doi.org/10.1016/j.engfailana.1.2013.02.009>
- Magliulo G, Ercolino M, Petrone C, Coppola O, Manfredi G (2014a) The Emilia earthquake: seismic performance of precast reinforced concrete buildings. *Earthq Spectra* 30(2):891–912. <https://doi.org/10.1193/091012EQS285M>
- Magliulo G, Ercolino M, Cimmino M, Capozzi V, Manfredi G (2014b) FEM analysis of the strength of RC beam-to-column dowel connections under monotonic actions. *Constr Build Mater* 69:271–284. <https://doi.org/10.1016/j.conbuildmat.2014.07.036>
- Magliulo G, Ercolino M, Manfredi G (2015) Influence of cladding panels on the first period of one-story precast buildings. *Bull Earthq Eng* 13(5):1531–1555. <https://doi.org/10.1007/s10518-014-9657-2>
- McKenna F (2011) OpenSees: a framework for earthquake engineering simulation. *Comput Sci Eng* 13(4):58–66. <https://doi.org/10.1109/MCSE.2011.66>
- Menegotto M, Pinto PE (1973) Method of analysis for cyclically loaded reinforced concrete plane frames including changes in geometry and non-elastic behaviour of elements under combined normal force

- and bending. In: IABSE symposium of resistance and ultimate deformability of structures acted on by well-defined repeated loads, vol 13. International Association of Bridge and Structural Engineering, pp 5–22
- NP EN 1992-1-1:2010. Eurocode 2: design of concrete structures-part 1-1: general rules and rules for buildings. Instituto Português da Qualidade
- Ozderem A, Barakat S (2000) After the Marmara earthquake: lessons for avoiding short cuts to disasters. *Third World Q* 21(3):425–439. <https://doi.org/10.1080/01436590050057717>
- Priestley M, Calvi M, Kowalsky M (2007) Displacement-based seismic design of structures. Pavia
- Rodrigues D, Crowley H, Silva V (2018) Earthquake loss assessment of precast RC industrial structures in Tuscany (Italy). *Bull Earthq Eng* 16(1):203–228. <https://doi.org/10.1007/s10518-017-0195-6>
- Rodrigues H, Sousa R, Vitorino H, Batalha N, Varum H, Fernandes P (2020) Characterisation of Portuguese RC precast industrial building stock. *Adv Civ Eng* 2020:7517205. <https://doi.org/10.1155/2020/7517205>
- Romão X, Costa AA, Paupério E, Rodrigues H, Vicente R, Varum H, Costa A (2013) Field observations and interpretation of the structural performance of constructions after the 11 May 2011 Lorca earthquake. *Eng Fail Anal* 34:670–692. <https://doi.org/10.1016/j.engfailanal.2013.01.040>
- RSA (1983) Regulamento de Segurança e Acções para Estruturas de Edifícios e Pontes - Decreto-Lei n.º 235/83
- Scott RPB, Priestley MJN (1982) Stress–strain behavior of concrete confined by overlapping hoops at low and high strain rates. *J Proc* 79(1):13–27. <https://doi.org/10.14359/10875>
- Senel SM, Kayhan AH (2010) Fragility based damage assesment in existing precast industrial buildings: a case study for Turkey. *Struct. Eng Mech* 34(1):39–60. <https://doi.org/10.12989/sem.2010.34.1.039>
- Sezen H, Whittaker A (2006) Seismic performance of industrial facilities affected by the 1999 Turkey earthquake. *J Perform Constr Facil* 20:28–36
- Silva V, Crowley H, Varum H, Pinho R, Sousa L (2015) Investigation of the characteristics of Portuguese regular moment-frame RC buildings and development of a vulnerability model. *Bull Earthq Eng* 13(5):1455–1490. <https://doi.org/10.1007/s10518-014-9669-y>
- Sousa R, Almeida JP, Correia AA, Pinho R, Modelling FF (2018) Shake table blind prediction tests: contributions for improved fiber-based frame modelling. *J Earthq Eng* 00(00):1–42. <https://doi.org/10.1080/13632469.2018.1466743>
- Sousa R, Batalha N, Rodrigues H (2020) Numerical simulation of beam-to-column connections in precast reinforced concrete buildings using fibre-based frame models. *Eng Struct* 203:109845

**Publisher's Note** Springer Nature remains neutral with regard to jurisdictional claims in published maps and institutional affiliations.